

## Supporting Information

### Dielectric Constant Engineering of Organic Semiconductors: Effect of Planarity and Conjugation Length

Wei Jiang,<sup>1</sup> Hui Jin,<sup>1</sup> Mohammad Babazadeh,<sup>1</sup> Alex S. Loch,<sup>1</sup> Aaron Raynor,<sup>1</sup> Neil Mallo,<sup>1</sup> David M. Huang,<sup>2</sup> Xuechen Jiao,<sup>3</sup> Wen Liang Tan,<sup>3</sup> Christopher R. McNeill,<sup>3</sup> Paul L. Burn,<sup>1\*</sup> Paul E. Shaw<sup>1</sup>

<sup>1</sup> Centre for Organic Photonics & Electronics (COPE), School of Chemistry and Molecular Biosciences, The University of Queensland, Brisbane, QLD 4072, Australia

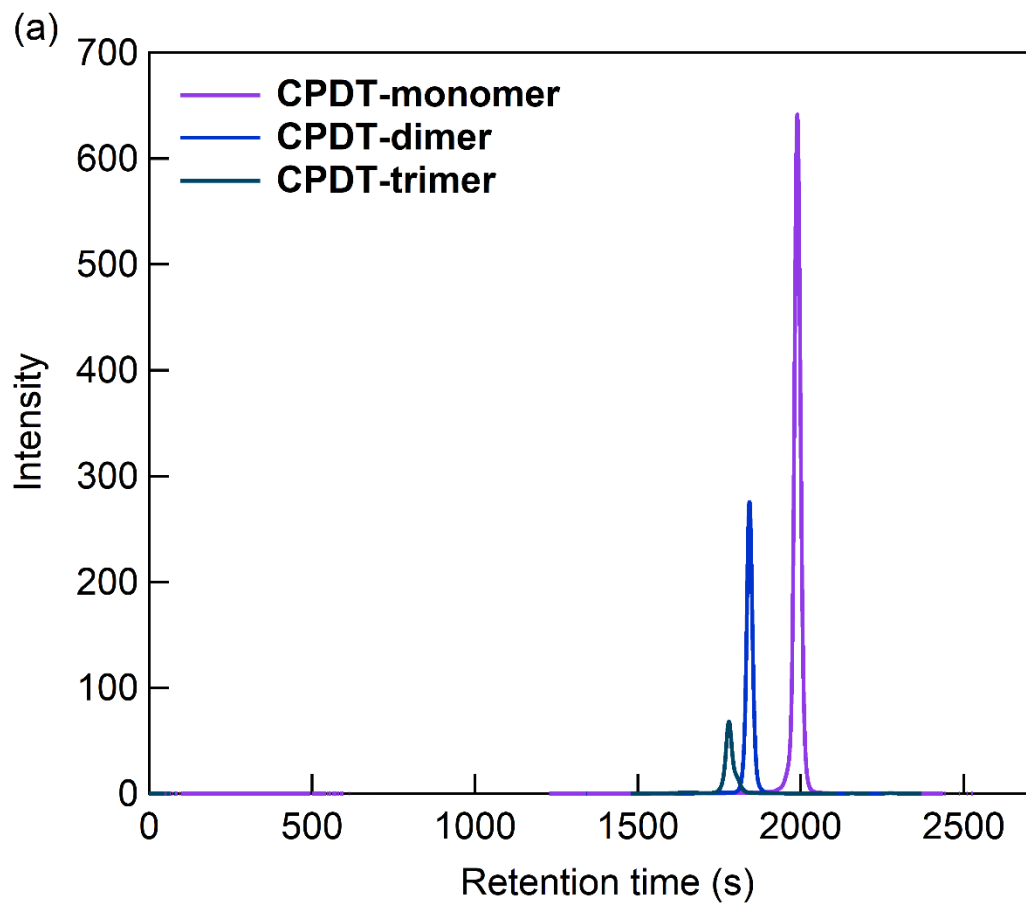
<sup>2</sup> Department of Chemistry, School of Physical Sciences, The University of Adelaide, Adelaide South Australia, 5005, Australia

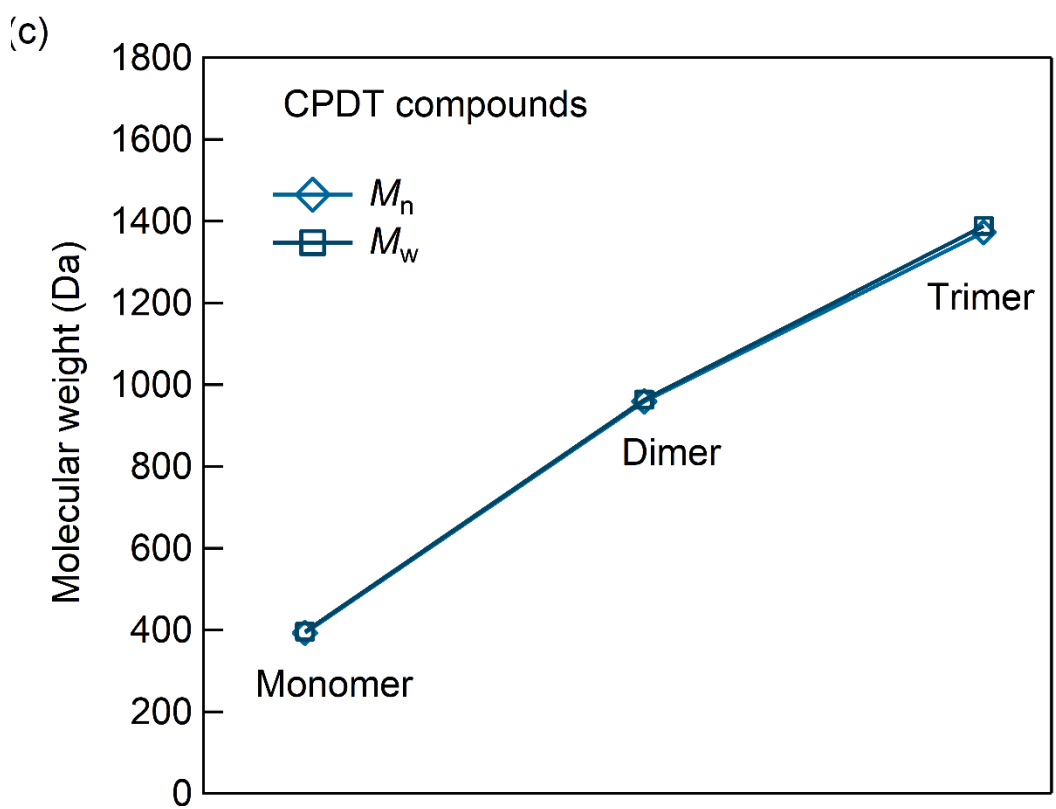
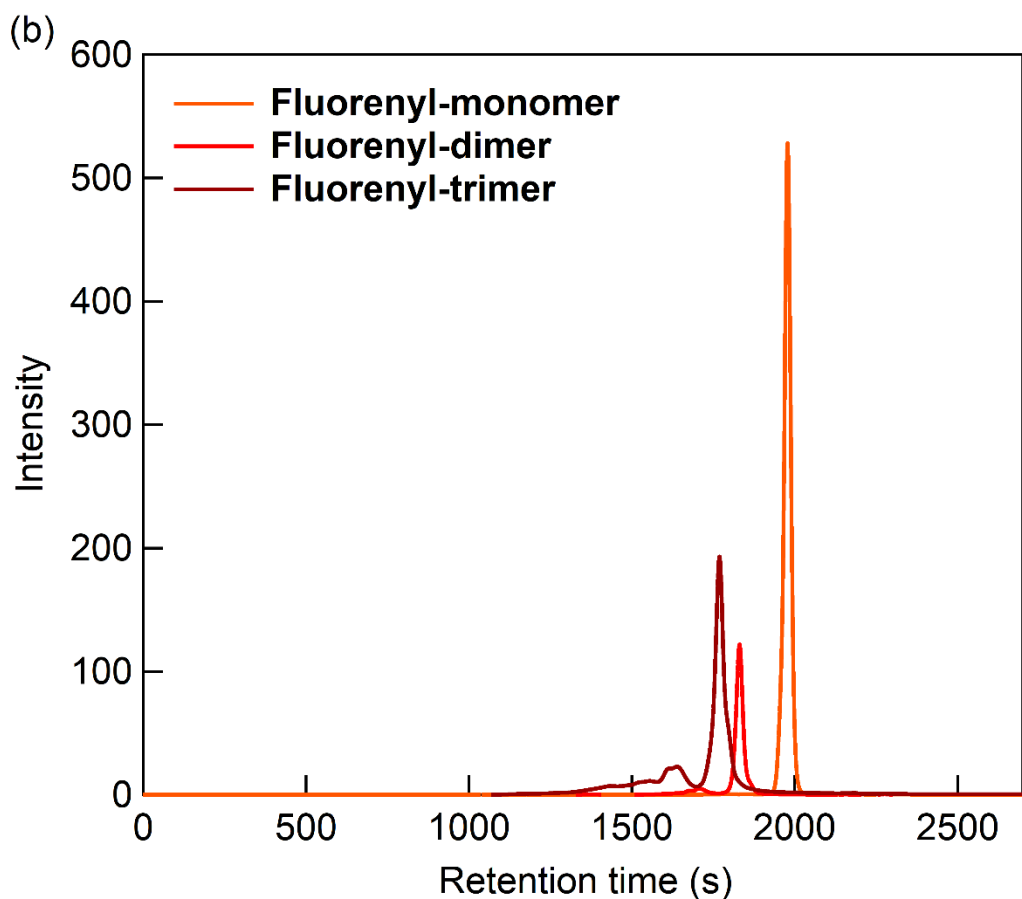
<sup>3</sup> Department of Materials Science and Engineering, Monash University, Clayton, Victoria 3800, Australia

#### 2-Bromo-7-iodo-9,9-bis[2-(2-methoxyethoxy)ethyl]-9H-fluorene

A mixture of 2-bromo-7-iodo-9*H*-fluorene<sup>[1]</sup> (3.00 g, 8.1 mmol), 2-(2-methoxyethoxy)ethyl-4-methylbenzenesulfonate<sup>[2]</sup> (5.70 g, 20.8 mmol), and potassium hydroxide (1.30 g, 23.2 mmol) in anhydrous *N,N*-dimethylformamide (35 mL) was heated at 60 °C under argon overnight in the dark. The solution was allowed to cool to room temperature and diluted with hydrochloric acid (3M, 100 mL) and ethyl acetate (30 mL). The aqueous layer was isolated and extracted with ethyl acetate (3 × 30 mL). The combined organic fractions were washed with deionized water (3 × 30 mL), brine (2 × 30 mL), dried over anhydrous sodium sulfate, filtered through a silica plug, and the solvent was removed. The crude product was purified using flash column chromatography over silica with ethyl acetate:*n*-hexane mixtures (0:1 to 1:1) as eluent to yield 2-bromo-7-iodo-9,9-bis[2-(2-methoxyethoxy)ethyl]-9*H*-fluorene as a colourless oil, which solidified overnight (3.60 g, 77%); m.p.: 54 °C; found: C, 47.9; H, 4.9; C<sub>23</sub>H<sub>28</sub>BrIO<sub>4</sub> requires: C, 48.0; H, 4.9; λ<sub>max</sub> (CH<sub>2</sub>Cl<sub>2</sub>/nm): 275 sh (log ε/dm<sup>3</sup> mol<sup>-1</sup> cm<sup>-1</sup> 4.74), 287 (4.80), 304 (4.62), 316 (4.67); δ<sub>H</sub> (500 MHz, CDCl<sub>3</sub>): 2.34-2.37 (4H, m, Gl-CH<sub>2</sub>), 2.75-2.78 (4H, m, Gl-CH<sub>2</sub>), 3.18-3.20 (4H, m, Gl-CH<sub>2</sub>), 3.28-3.32 (10H, m, Gl-CH<sub>2</sub> and Gl-CH<sub>3</sub>), 7.39 (1H, dd, *J* = 0.5, 8.0 Hz, Fl-H), 7.46 (1H, dd, *J* = 1.5, 8.0 Hz, Fl-H), 7.51 (1H, dd, *J* = 0.5, 8.0 Hz, Fl-H), 7.54 (1H, dd, *J* = 0.5, 1.5 Hz, Fl-H), 7.67 (1H, dd, *J* = 1.5, 8.0 Hz, Fl-H), 7.74 (1H, dd, *J* = 0.5, 1.5 Hz, Fl-H); δ<sub>C</sub> (125 MHz, CDCl<sub>3</sub>): 39.4, 51.8, 59.0, 66.8, 70.0, 71.7, 93.1, 121.2, 121.5, 121.8, 126.7, 130.6, 132.6, 136.5, 138.5, 139.0, 150.6, 151.0; *m/z* (ESI-HRMS) anal. calcd. for

$C_{23}H_{29}BrIO_4$   $[M + H]^+$ : 575.0288 (99%), 576.0322 (25%), 577.0271 (100%), 578.0303 (25%);  
found: 575.0287 (100%), 576.0324 (25%), 577.0268 (99%), 578.0301 (24%).





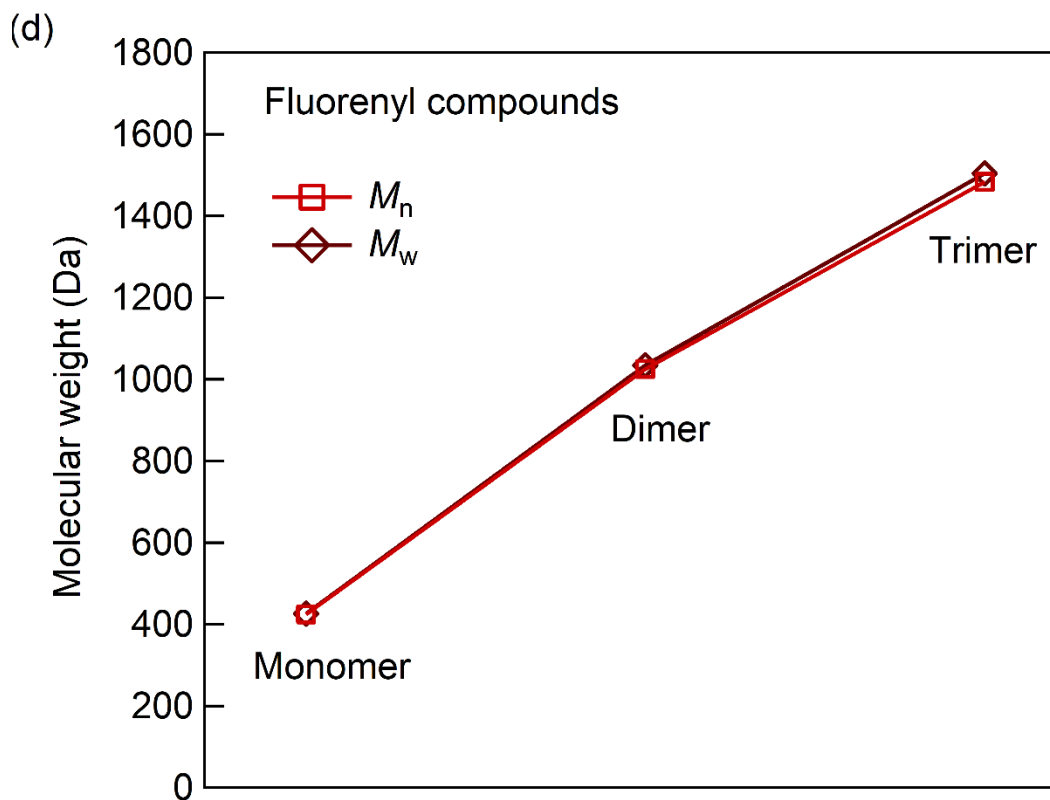


**Figure S1.** Gel Permeation Chromatography (GPC) traces and analysis of the (a) CPDT compounds, (b) Fluorenyl compounds, and plots of  $\bar{M}_n$  and  $\bar{M}_w$  for (c) CPDT compounds and (d) Fluorenyl compounds showing that the materials are monodisperse. The **Fluorenyl-trimer** was found to have lower solubility in the tetrahydrofuran used for the measurement. **Figure S2** shows that the higher molecular weight component was concentration dependent (larger at high concentration) and hence arose from aggregation. Estimation of molecular weights by GPC was carried out using an Agilent 1260 Infinity II system equipped with a variable wavelength detector set to 360 nm, two PLgel Mixed-E columns (600 mm + 300 mm lengths, 7.5 mm diameter) from Polymer Laboratories, calibrated with polystyrene narrow standards ( $\bar{M}_p = 162$  to 47,190 gmol<sup>-1</sup>) and run in series in tetrahydrofuran with toluene as flow marker. The tetrahydrofuran pumped at a rate of 0.5 mL min<sup>-1</sup> with the columns maintained at 40 °C.

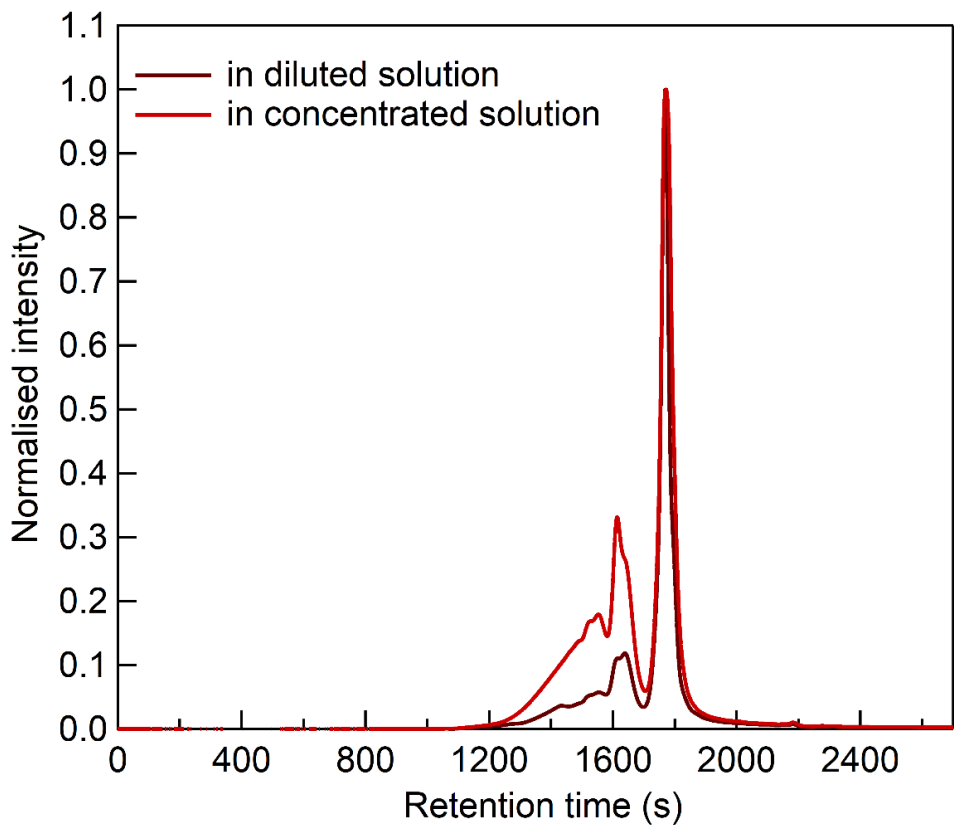


**Figure S2.** Normalized GPC traces for the **Fluorenyl-trimer** at different concentrations.

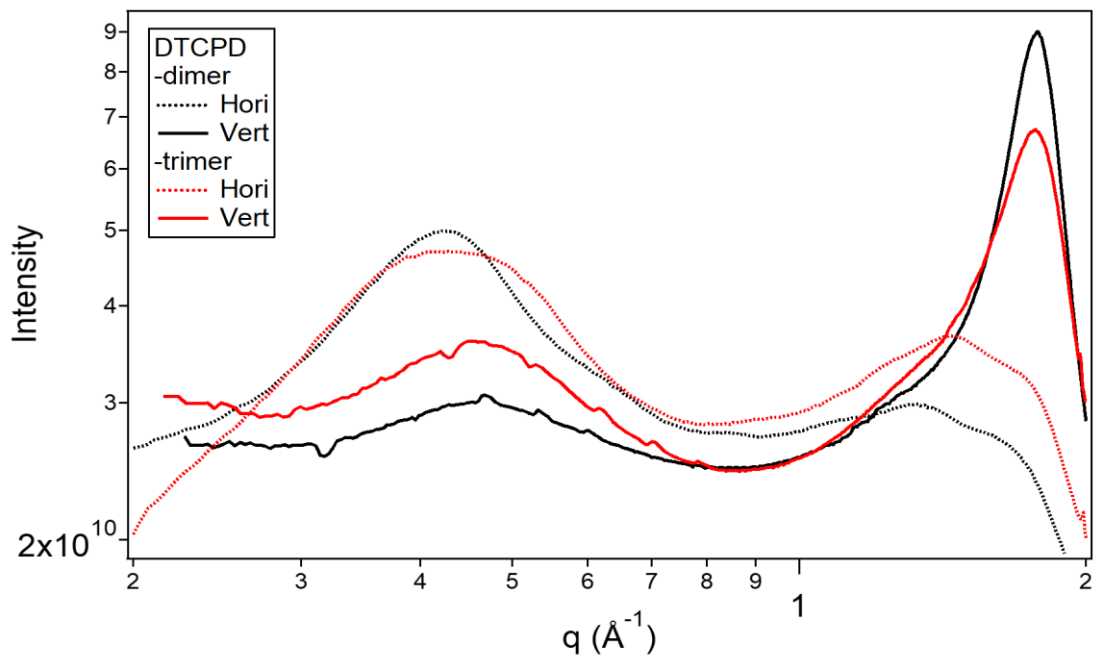
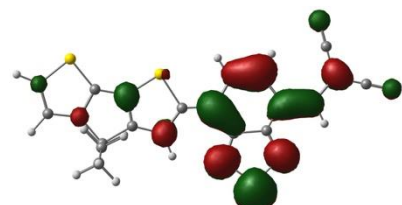


**Figure S3.** Comparison of in-plane (dotted) and out-of-plane (solid) one-dimensional scattering profiles of the **CPDT-dimer** (black) and **CPDT-trimer** (red).

**Table S1.** Energy,  $E$ , wavelength,  $\lambda$ , and oscillator strength,  $f$ , from TD-DFT calculations of lowest energy singlet absorption transition of monomer, dimer, and trimer of CPDT and fluorenyl series in the gas phase and a dielectric medium (corresponding to dichloromethane).

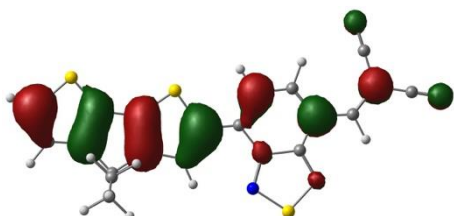
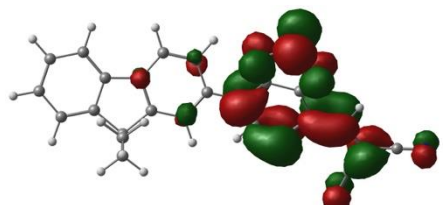
		gas phase		dielectric medium	
		$E$ (eV) / $\lambda$ (nm)	$f$	$E$ (eV) / $\lambda$ (nm)	$f$
CPDT	monomer	2.241 / 553	1.2	2.111 / 587	1.5
	dimer	1.609 / 771	3.2	1.462 / 848	3.5
	trimer	1.445 / 858	3.1	1.304 / 951	3.4
fluorenyl	monomer	2.413 / 514	0.6	2.331 / 532	0.8
	dimer	2.103 / 590	1.1	2.019 / 614	1.3
	trimer	1.958 / 633	0.8	1.912 / 649	0.9

**CPDT-monomer**

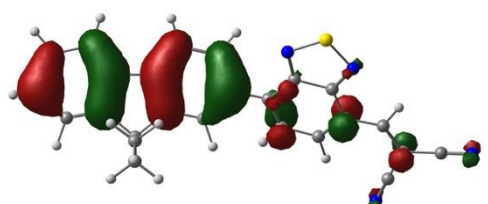


**Electron**

**Fluorenyl-monomer**

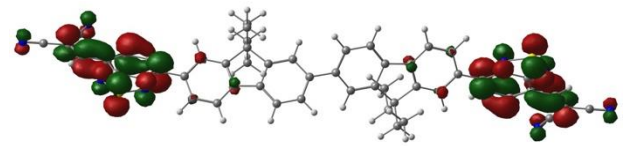
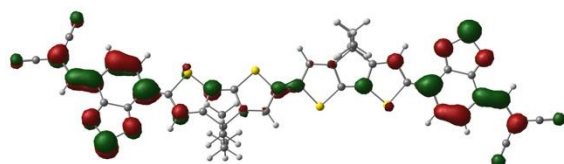


**Hole**



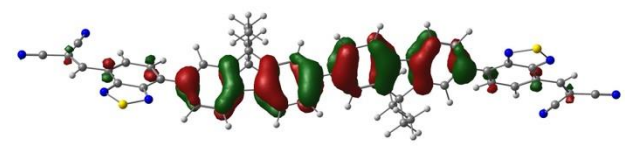
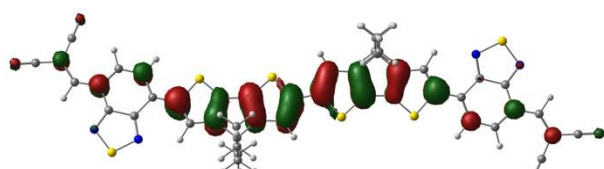
**CPDT-dimer**

**Fluorenyl-dimer**



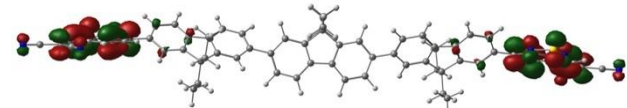
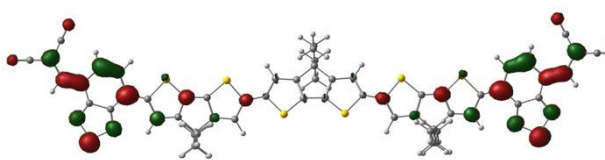
**Electron**

**Hole**



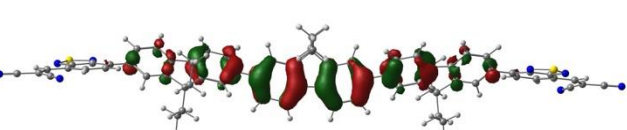
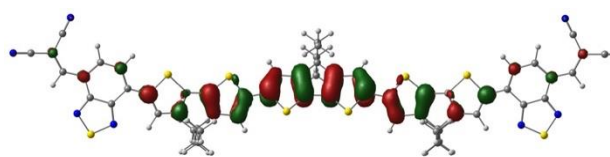
**CPDT-trimer**

**Fluorenyl-trimer**

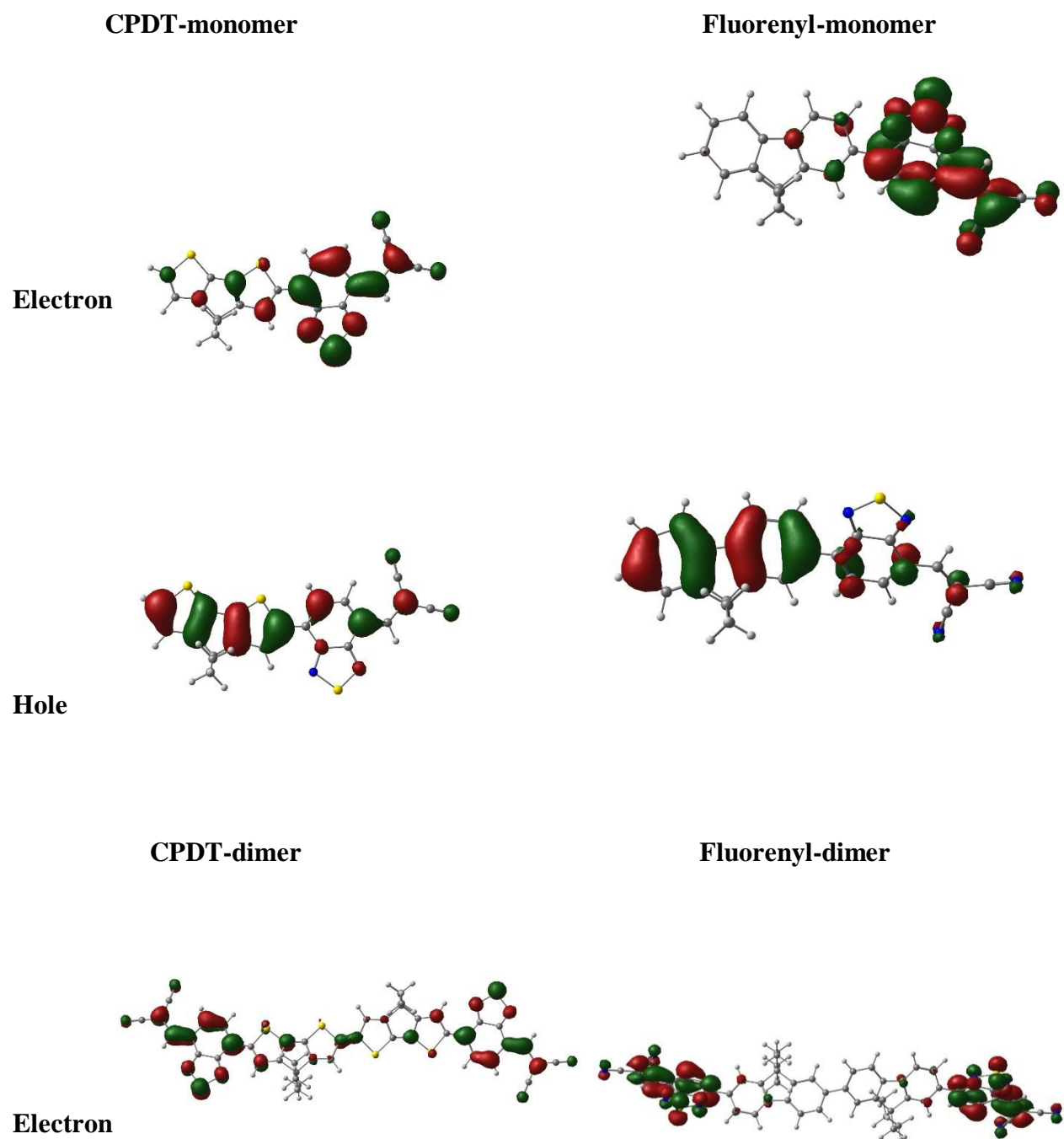


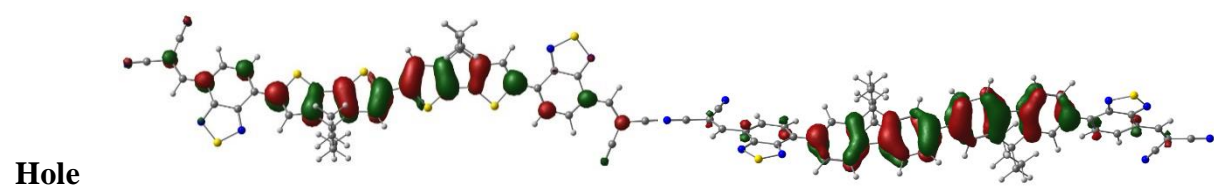
**Electron**

**Hole**



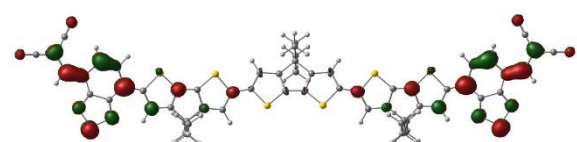
**Figure S4.** Natural transition orbitals (isovalue = 0.03 e/bohr<sup>3</sup>) for lowest energy absorption transition from TD-DFT calculations (gas phase).





**CPDT-trimer**

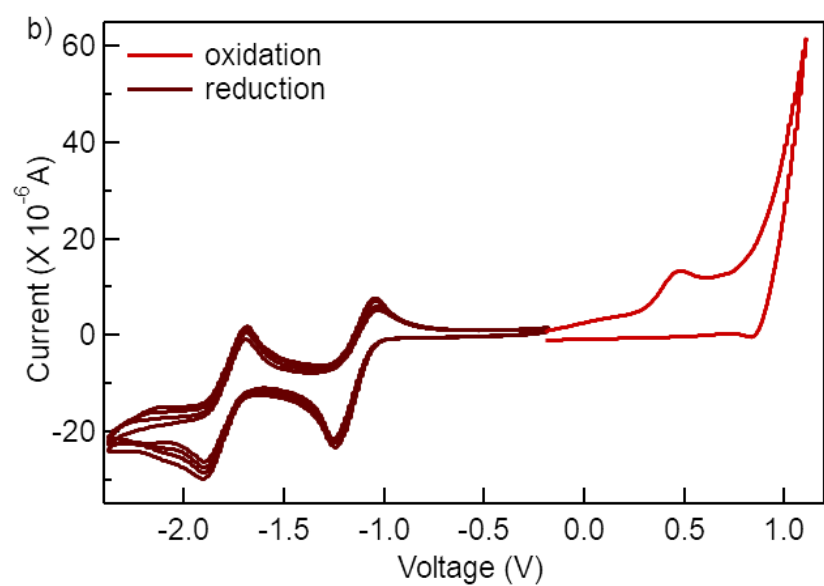
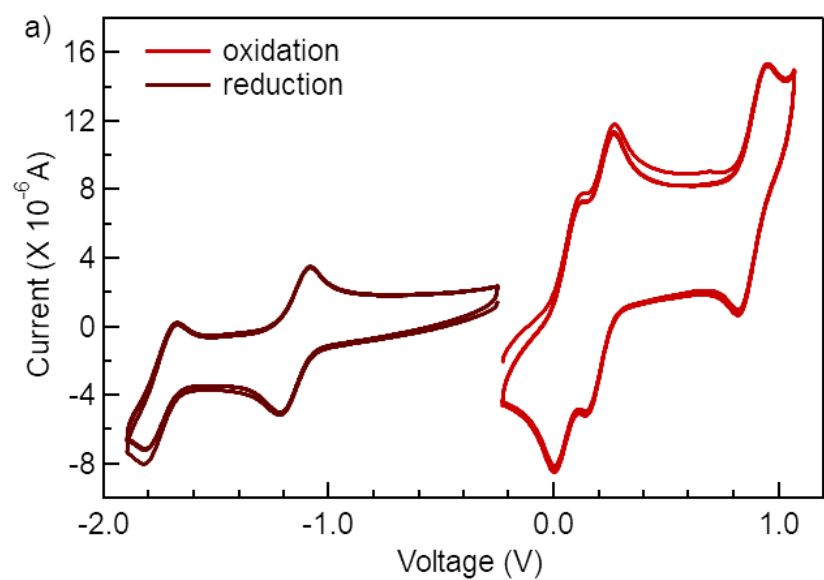
**Fluorenyl-trimer**



**Electron**



**Figure S5.** Natural transition orbitals (isovalue = 0.03 e/bohr<sup>3</sup>) for lowest energy absorption transition from TD-DFT calculations (dielectric medium).



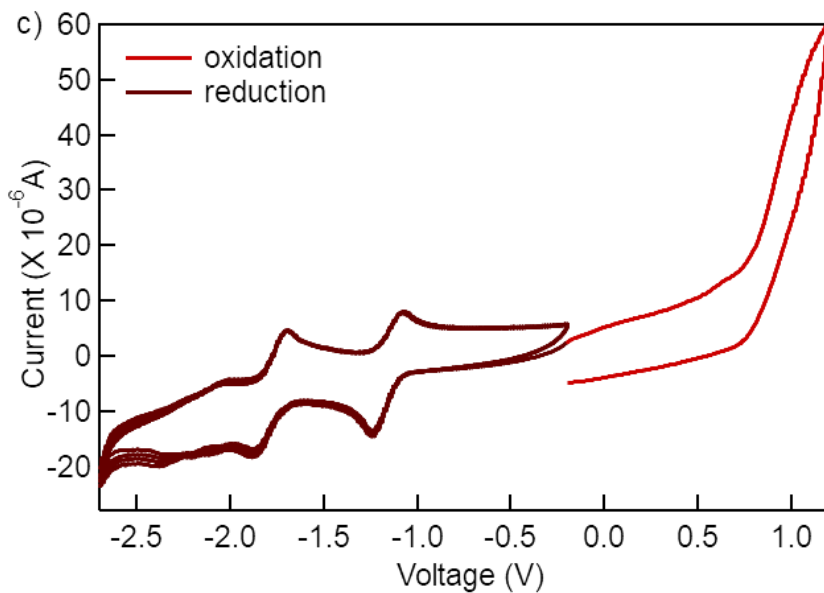


**Figure S6.** Cyclic voltammograms of a) **CPDT-trimer** (scan rate: 100 mV/s), b) **Fluorenyl-dimer** (scan rate: oxidation: 50 mV/s, reduction: 100 mV/s), c) **Fluorenyl-trimer** (scan rate: 100 mV/s). All the measurements were performed in tetrahydrofuran with the  $E_{1/2}$ s quoted against the Ferrocene/Ferrocenium couple using tetra-*n*-butylammonium perchloride as the electrolyte. The oxidations of both the **Fluorenyl-dimer** and **-trimer** are neither chemically nor electrochemically reversible, so only the first scanning cycle is shown. Cyclic voltammograms of the **CPDT-dimer** have been reported elsewhere.<sup>[3]</sup>

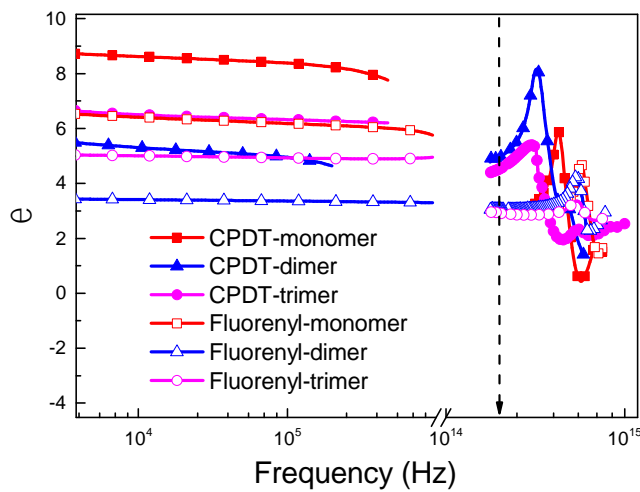


**Figure S7.** Dielectric constants of the materials *versus* frequency.

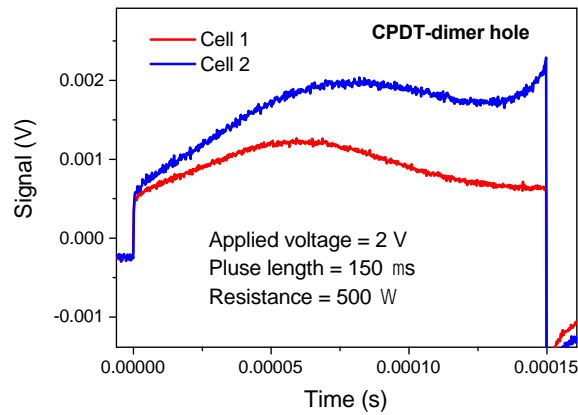
**Table S2.** Film-thickness dependent optical-frequency dielectric constant ( $\epsilon_{\text{opt}}$ ) of CPDT-compounds.

$\epsilon_{\text{opt}}$  of CPDT-compounds

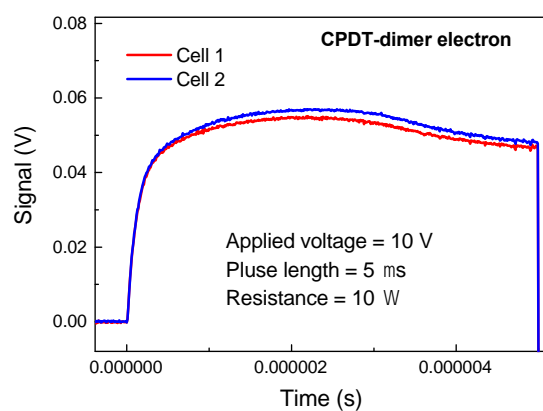
Film thickness (nm)

	monomer	dimer	trimer
20-30	3.2	5.8	4.4
35-45	3.4	5.2	4.3
> 50	3.2	4.6	4.6

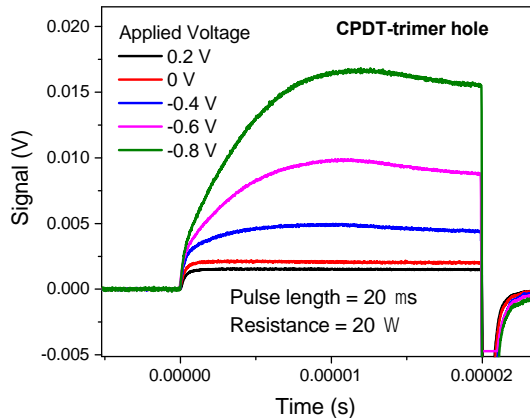
(a)



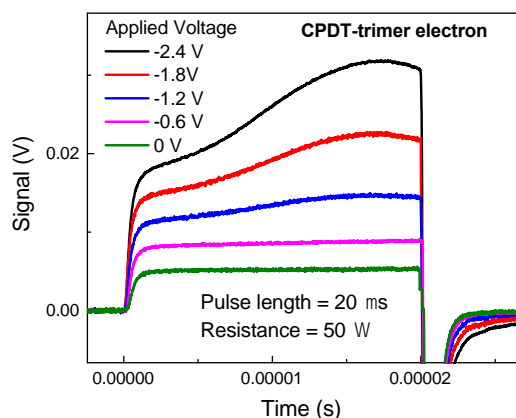
(b)



(c)

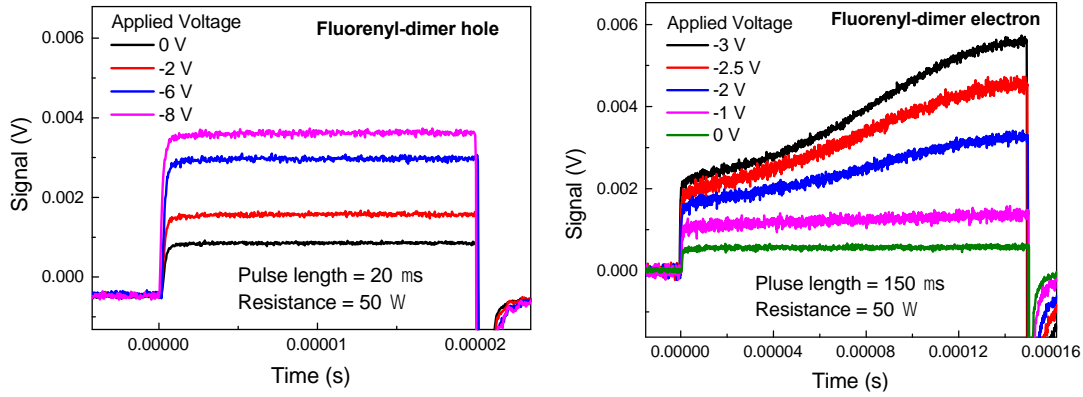


(d)



(e)

(f)



(g)

(h)

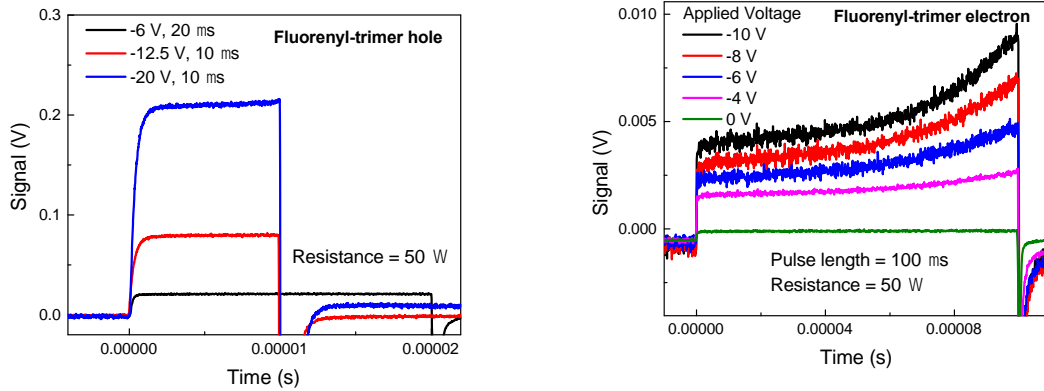
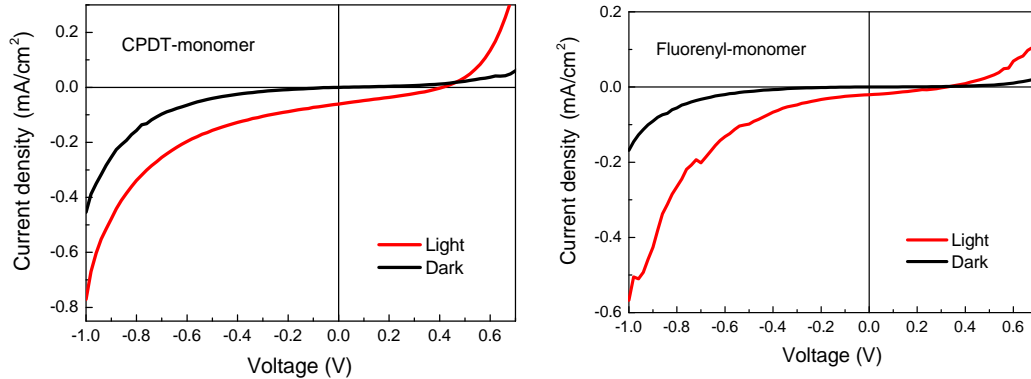


**Figure S8.** Hole and electron mobilities for the **CPDT-dimer** (a and b) and **-trimer** (c and d), and **Fluorenyl-dimer** (e and f) and **-trimer** (g and h) using Metal-Insulator-Semiconductor Charge Extraction by Linear Increasing Voltage (MIS-CELIV).

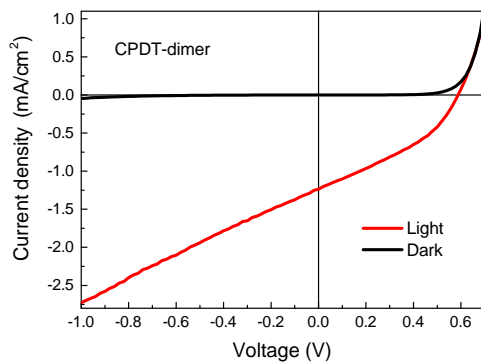
(a)

(d)

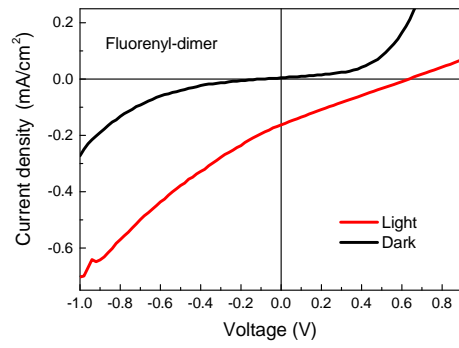


(b)

(e)



(c)



(f)

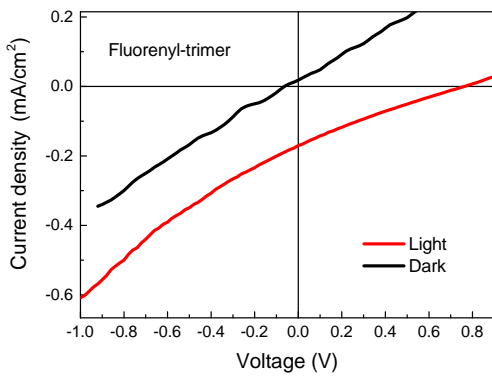
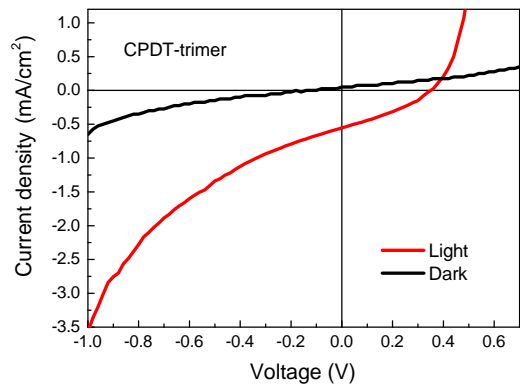


**Figure S9.** Current density versus voltage ( $J$ - $V$ ) characteristics in the dark and under illumination of  $100 \text{ mW}/\text{cm}^2$  for devices composed of the **CPDT-monomer** (a), **-dimer** (b) and **-trimer** (c), and **Fluorenyl-monomer** (d), **-dimer** (e) and **-trimer** (f).

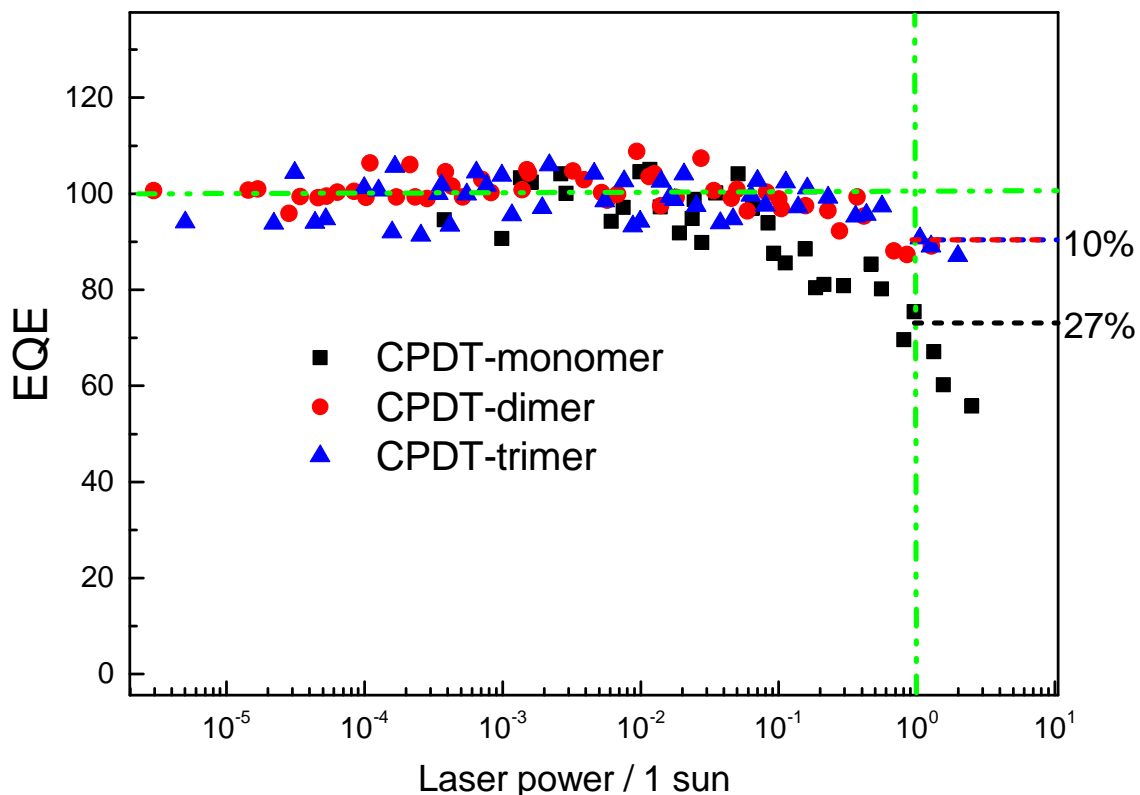


**Figure S10.** Normalized External Quantum Efficiencies (EQE) as a function of the laser power/1 sun (532 nm), with the 1 sun equivalent laser power marked as a green dashed line, at short-circuit conditions for the CPDT-based homojunction devices. The deviation from the linear photocurrent/constant EQE dependence allows estimation of the bimolecular recombination losses at a 1 sun equivalent power.

#### References:

- [1] M. P. Aldred, P. Vlachos, A. E. A. Contoret, S. R. Farrar, W. Chung-Tsoi, B. Mansoor, K. L. Woon, R. Hudson, S. M. Kelly, M. O'Neill, *J. Mater. Chem.* **2005**, *15*, 3208.
- [2] Z. Jia, W. Yuan, C. Sheng, H. Zhao, H. Hu, G. L. Baker, *J. Polym. Sci. Part A: Polym. Chem.* **2015**, *53*, 1339.
- [3] A. Armin, D. M. Stoltzfus, J. E. Donaghey, A. J. Clulow, R. C. R. Nagiri, P. L. Burn, I. R. Gentle, P. Meredith, *J. Mater. Chem. C* **2017**, *5*, 3736.